JOURNAL OF MATERIALS SCIENCE 27 (1992) 4591–4597

# Characterization of the interface in a carbon–epoxy composite using transmission electron microscopy

M. GUIGON
*Division Polymères et Composites. BP 649, Universite de Technologie, 60206 Compiegne Cedex, France*

Two commercial kinds of unsized pan-based carbon fibres (high strength and high modulus) were subjected to electrochemical treatments (oxidative and non-oxidative) and to a nitrogen plasma. After embedding in an epoxy resin, they were sectioned by ultramicrotomy (diamond knife), and the interface between the resin matrix and the fibre was studied by the lattice fringes method (TEM). The adhesion of the fibre to the matrix depends on the surface treatment and the external microtexture of the fibre. High-modulus fibres (plasma etching) show a good adhesion only when the carbon layers are perpendicular to the interface. High-strength fibres exhibit two types of adhesion. Some treatments yield a surface which mainly presents carbon layers parallel to the interface with a rugosity of about 1–2 nm. The second type of adhesion consists of fibre–matrix interpenetration. In this case carbon layers are slightly exfoliated and perpendicular to the interface. For most treatments, interfacial shear stress was determined by the pull-out test. We found no correlation between TEM observations and shear stress data. Consequently, we were unable to discuss adhesion from the transmission electron microscopy results. It would probably be more reliable to consider the problem with a concept based on interface toughness. However, as a first step, we have defined a new parameter, the "contact index", and have shown the relations between the contact index, the morphology of the interface and the interfacial shear stress determined by the pull-out test.

## 1. Introduction

It is well known that in a composite material the charge transfer is only carried out if the fibre–matrix bonding is such that shear stresses due to the difference between the elastic modulus of the two components does not lead to interface decohesion.

The resilience of a composite material depends partially on the fibre–matrix adhesion. A material is resilient when the stored elastic energy can be consumed by various processes of fibre–matrix decohesion. We can thus find some examples of high-strength composites with weak resilience. The optimization of the adhesion would consist in having a high strength related to a high resilience. Therefore, we see the importance of an accurate characterization of the fibre–matrix interface.

We have studied the fibre–matrix junctions by the lattice fringes method (transmission electron microscopy). The mechanical test (pull-out test) was carried out at ONERA.

## 2. Role and characterization of the fibre–matrix interface

A large number of tests have been developed for evaluating the shear strength of the interface. All these tests are related to the destruction of the fibre–matrix bonding [1–9]. The selected test is the pull-out test which was carried out at ONERA [8]. All the mechanical tests done for the characterization of the adhesion do not show whether the fracture is produced at the fibre–matrix interface or inside one component of the composite. The answer to this question could be found if only we could carry out the fine characterization of the interface without interfering with the sample between the mechanical testing and the interface characterization. Unfortunately, this problem has not been solved yet.

The interface is specific for a given fibre–matrix system. However, we can generalize a few points which can be applied to all the systems. The fibre–matrix adhesion depends on:

(i) the external characteristics of the fibre (fine structure, topography, surface energy, etc.);

(ii) the surface treatments of the fibre carried out for the fabrication of composites;

(iii) the nature of the matrix;

(iv) the chemical reactions between the fibre and the matrix; and

(v) the stress state of the fibre (mechanical hanging up, differential thermal dilatation coefficients, etc.).

Electron microscopy (scanning and transmission) gives us indications about the topography and the fine structure of the fibres. By ESCA we have access to the

0022–2461  

nature of the chemical functions present on the fibre surface. Unfortunately, no technique has been used to obtain simultaneously all this information.

Transmission electron microscopy, as used here, is relevant "to see" the fibre–matrix junctions but does not give access to the chemical functions, if they exist. Therefore, we propose to characterize various junctions as a function of different surface treatments of the fibres, according to the conditions and criteria defined.

## 3. Experimental conditions

### 3.1. The microscope

Fine structural details smaller than 1 nm were sought. In such cases samples must be used for which the variation of the phase $\varphi$ is small compared to the average phase $\varphi_o$ (weak phase object). For these conditions, the optical system, i.e. the transfer mechanisms, play an outstanding role in the formation of the images and their interpretation.

Let $\varphi_o$ and $\varphi_i$ be the complex amplitudes of the object and image waves, respectively. The relation of object to image is expressed as

$$\varphi_i = K \varphi_i \quad (1)$$

where $K$ is the impulsion response of the objective lens. This relation of convolution is equivalent to the relation of transfer

$$\boldsymbol{\varphi}_i = \mathbf{K}\boldsymbol{\varphi}_o \quad (2)$$

($\boldsymbol{\varphi}_i$, $\mathbf{K}$, $\boldsymbol{\varphi}_o$ are the Fourier transforms of $\varphi_i$, $K$, $\varphi_o$).

Lannes and Perez [10] showed that the transfer function is

$$\mathbf{K}(u) = D(\lambda f u) \exp - i\chi(u) \quad (3)$$

with

$$\chi(u) = \pi[\tfrac{1}{2}C_s\lambda^3 u^4 - \lambda\Delta f u^2] \quad (4)$$

$u$ is the spatial frequency, $\chi(u)$ is the aberration function, $D$ is the characteristic function of the objective aperture and $\Delta f$ is the defocusing.

Thus we can state that the wavelength, $\lambda$, and the spherical aberration, $C_s$, play an important role in a microscope. The objective lens behaves like a filter for spatial frequencies that selects and modifies the phase of planar waves that can interfere in the image plane. We used an axial mode and a partially coherent illumination. It is shown that in these conditions the transfer function of a phase contrast is, in first approximation, proportionate to $-2 \sin \chi(u)$.

For our studies we used the interference of the transmitted beams without deviation and the (0 0 2) beam diffracted by the carbon layers of the fibre. In the case of Courtaulds high-strength fibres studied here, $d_{0\,0\,2}$ is of the order of 0.36 nm, corresponding to a peak centred on 2.8 $nm^{-1}$ with a half-maximum-intensity width of 0.5 $nm^{-1}$ for a thickness of five carbon layers. In the case of high-modulus fibres, the peak is centred on 2.9 $nm^{-1}$ ($d_{0\,0\,2}$ = 0.345 nm) (stack of ten carbon layers) [11].

Therefore, from these data, it became necessary to seek a value of $\Delta f$ defocalization in order to obtain an optimal value of the transfer function in the frequency band 2.3–3.3 $nm^{-1}$. The values satisfying $\Delta f$ = 72 nm (under focus) are, in our case, very near Scherzer's conditions. A graph of this function is shown in Fig. 1.

### 3.2. The sample

The sample must be very thin to be considered a weak phase object. Ultramicrotomy was employed to prepare very thin sections. The unsized but treated fibres were embedded in an epoxy resin and the sample was cut perpendicular to the fibre axis with a diamond knife: the sections were 50–80 nm thick. Fig. 2 shows a section of a high-modulus fibre. The problems of degradation associated with ultramicrotomy are illustrated in this figure (vibration of the blade during its passage through materials of different hardness).

### 3.3. Criteria of the thin sections

First, thin sections were chosen on the basis of their quality, at low magnification. They were then confirmed to be transverse sections by examining the morphology of the carbons layers at high magnification [11].

### 3.4. Definitions

The electron microscope gives a two-dimensional image from a three-dimensional object. Therefore, in

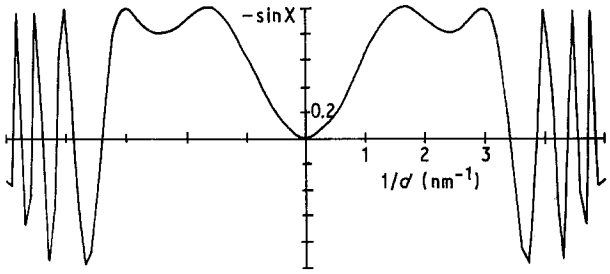


*Figure 1* Transfer function with $\Delta f$ = 72 nm.

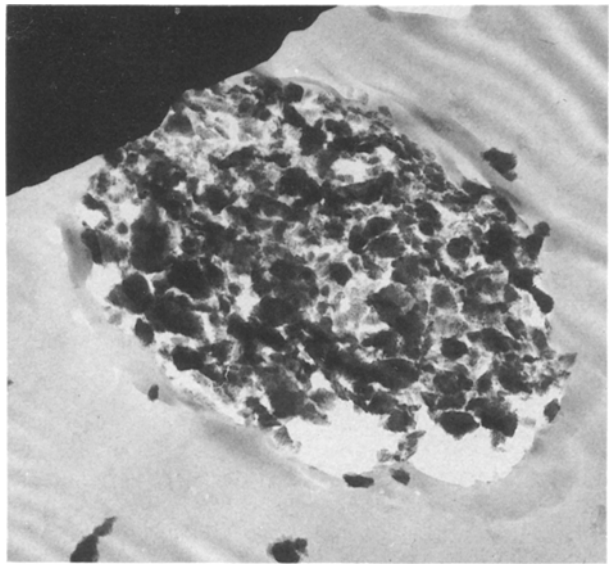

*Figure 2* High-modulus fibre section obtained by ultramicrotomy.

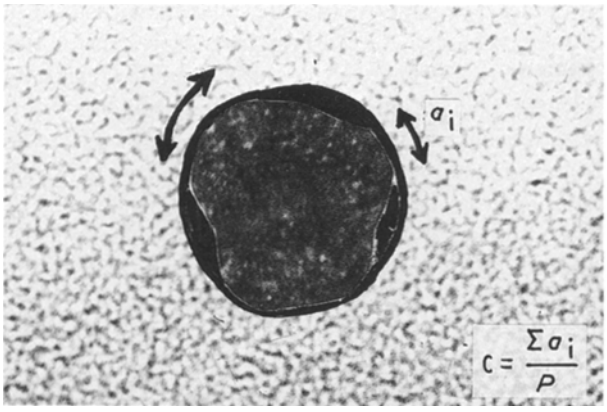


*Figure 3* Definition of the "contact index".

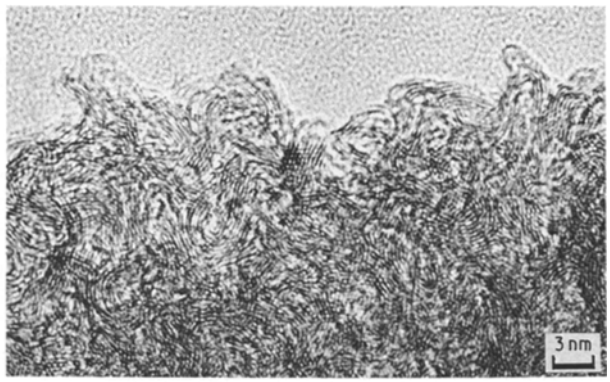


*Figure 4* Typical texture of a high-strength carbon fibre.

our case, the contact ratio of the fibre with the matrix is related to the length of the interface and is obviously correlated to the modified external structure of the fibre. Let us consider Fig. 3, where $a_i$ is the length of the fibre–matrix junction and $p$ the perimeter of the fibre. The "contact index" is defined as

$$C = \sum_i a_i/p \qquad (5)$$

### 3.5. Surface treatment

For industrial surface treatments (oxidizing treatments), chemical bonds are formed between the functional group introduced C–OH, C=O and COOH, and the amine group coming from the resin hardener.

The idea which was at the basis of surface treatment with amine groups assumed that the functional amine groups grafted on the fibre surface have to react directly with the epoxy group of the resin to give a strong cohesion at the fibre–matrix interface. Based on this, Waltersson [12] recommended the treatment of carbon fibres with agents containing amine groups before using them in composite materials.

## 4. Materials and surface treatment used

High-strength and high-modulus fibres were used (Courtaulds fibres). The surface treatments with anodic and nitrogen plasma were carried out at ONERA [7, 8].

## 5. Results

### 5.1. Carbon fibres

We were able to identify the typical texture of carbon fibres (Fig. 4) [11, 13, 14]. They are made of carbon layers, whose length, stacking and radius of curvature depend on the fibre. However, in all cases, either the edge or the surface of the carbon layers can be exposed at the fibre surface.

High-strength fibres are characterized by a significant edge/surface distribution, whereas for high-modulus fibres the surface/edge distribution is a dominant character.

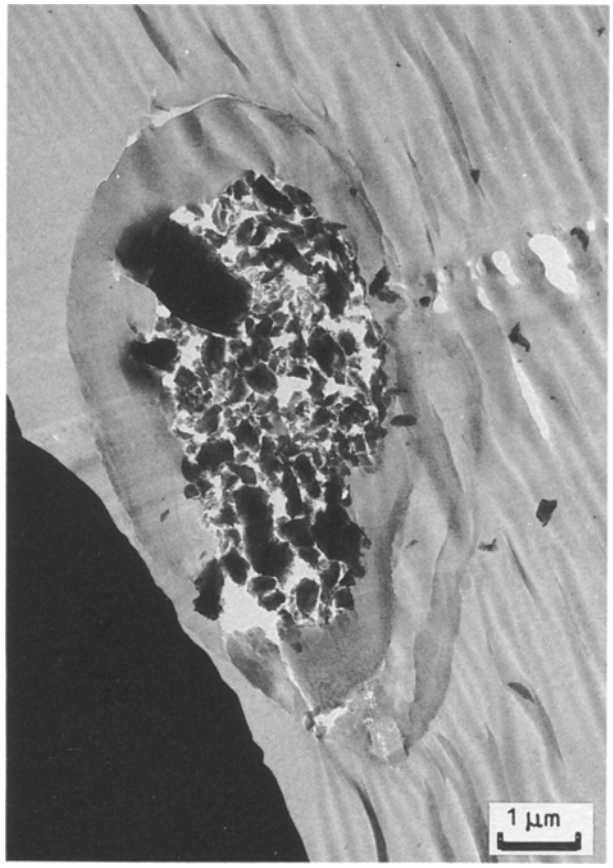


*Figure 5* Commercial fibre (Serofim 4225) with a strong sizing.

### 5.2. Oxidizing treatment

In commercial fibres we observed two phenomena:

(i) in the case of large sizing amounts (6%), an incompatible area between the sizing and the embedding resin (Fig. 5) was seen;

(ii) a transition area was observed between the fibre and the resin varying from 10–30 nm according to the topography of the fibre for weak sizings (Fig. 6). It is thought that this region might correspond to the interphase described by Drzal [15].

In the present work, carbon fibres were treated in an aqueous solution of $(NH_4)_2SO_4$ (anodic treatments). The treated fibres were directly embedded in the resin.

In all samples, no discontinuities were ever observed near the fibre surface.

Two types of junction were observed. When the treatment is weak (2 min, 1.18 V) there is a good

penetration of the carbon layers in the resin (the ionization potential of water is 1.75 V). The interface is thus diffused and seems to be a result of slightly exfoliated carbon layers (Fig. 7). The contact index is good. When the treatment is extended (2 min, 1.72 V), we observe a degradation of the fibres. Under the microscope, compared to the previous example, a smooth fibre surface can be seen. The carbon layers are preferentially oriented parallel to the fibre–matrix interface. We suppose that these layers withstood the attack, whereas the carbon layers presenting their edges to the surface were severely degraded (exfoliated layers). The presence of this preferential orientation was revealed by a large number of edges due to the superimposition of parallel carbon layers (Fig. 8). The contact index is poor, but it is not known if it exists in the composite or if it is due to the decohesion of the weak fibre–matrix junctions during the cutting process.

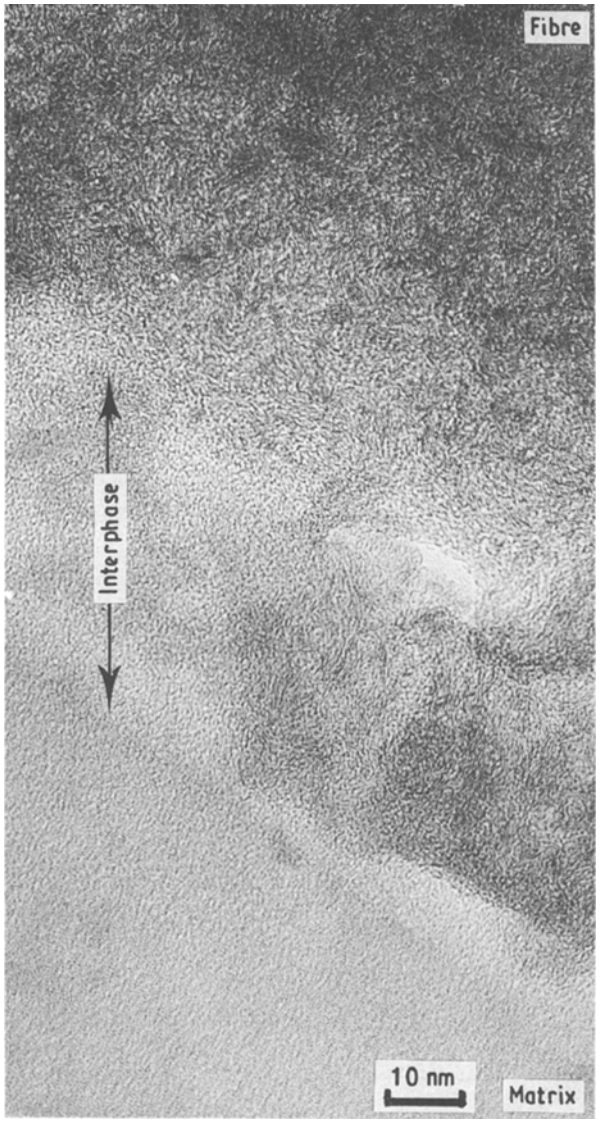


*Figure 6* Commercial fibre with a weak sizing (Courtaulds XAS).

## 5.3. Non-oxidizing treatments

All the samples were treated at a potential lower than the ionization potential of water (1.75 V).

### *5.3.1. Aqueous solution of tetramine hexamethylene (50 g $l^{-1}$): high-strength fibre*

Sample 1 (10 min, 1.45 V): this sample is characterized either by a good penetration of the carbon layer edges in the matrix without a clear interface (Fig. 9), or by an indented interface which gives a strong probability of carbon layers edges being at the interface (Fig. 10). In such a case, some circonvolutions present at the surface seem to favour the fibre–resin contact at depths varying from 2–5 nm. The contact index is high.

Sample 2 (1 h, 1.45 V): this sample shows a small percentage of fibre–matrix contact because there are

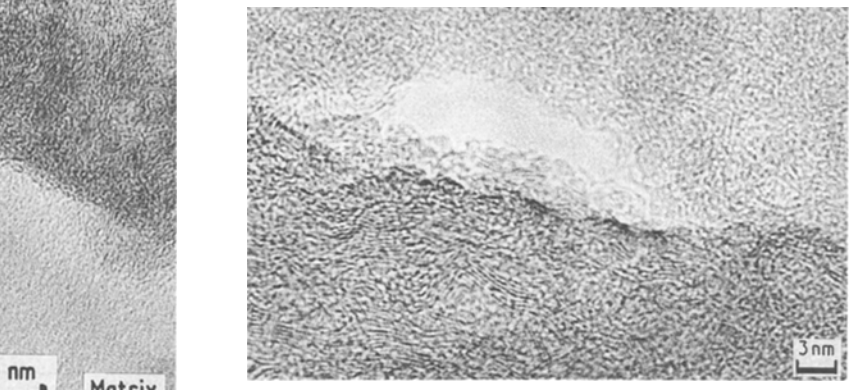


*Figure 8* High-strength carbon fibre: $(NH_4)_2SO_4$ treatment (2 min, 1.72 V).

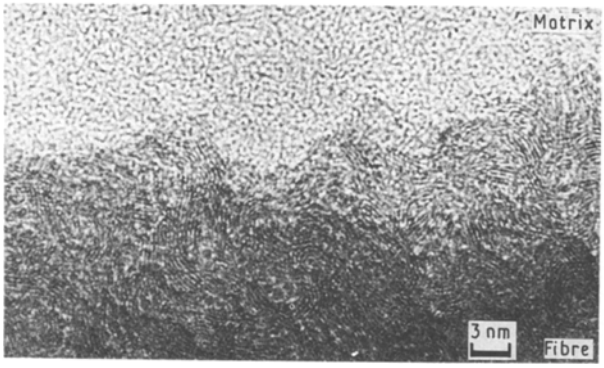


*Figure 7* High-strength carbon fibre: $(NH_4)_2SO_4$ treatment (2 min, 1.18 V).

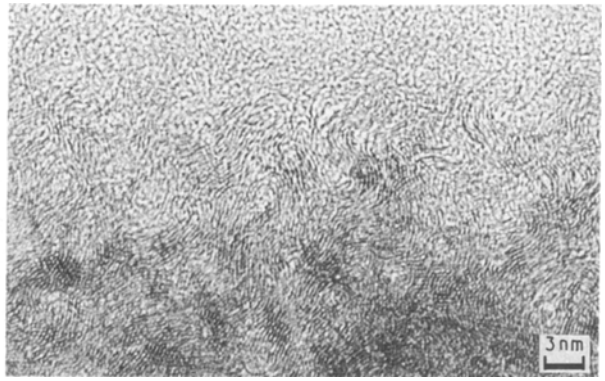


*Figure 9* High-strength carbon fibre: tetramine hexamethylene treatment (10 min, 1.45 V).

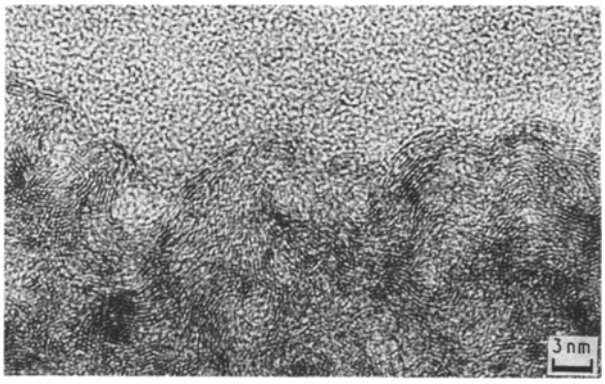


*Figure 10* High-strength carbon fibre: tetramine hexamethylene treatment (10 min, 1.45 V).

few areas of contact between the fibre and the matrix. However, when the junctions exist, they are perfect and of the type shown in Fig. 9. The contact index is low.

### 5.3.2. Aqueous solution of urea (50 g $l^{-1}$): high-strength fibre

Samples 1 (10 min, 1.5 V) and 2 (1 h, 1.5 V): these samples present either a perfect interface where the edges of the carbon layers are intimately attached to the resin (Fig. 11), or a long clear interface in which the surfaces of the layers are exposed at the interface (Fig. 12). We observed a type of non-linear border that could be a result of selective attack of the carbon layers. The convex area under tension is sensitive to chemical attack because of the presence of defects. The edges of the attacked layers are highly reactive regions, and undergo chemical reactions with the resin. On the contrary, the depressions (layers under compression) are less sensitive to the treatments and thus do not favour high fibre–matrix interactions.

The clear regions which were identified could be a result of the loading of depressions (weak adhesion) by the diamond knife and may be the beginning of a porosity at the interface. Note the presence of edges in the concave regions. This phenomenon is very often seen in high-modulus fibres and is due to a superimposition of carbon layers with their surfaces exposed to the interface. The presence of edges confirms that the concave regions are composed of parallel layers at the interface, which are not highly reactive. For such fibres, the contact index is good.

### 5.3.3. Nitrogen plasma: high-strength fibres (60 s) and high-modulus fibres (2 min, 30 s)

For all the treatments, the contact index is small and most of the junctions are formed with edges of the carbon layers (Figs 13 and 14).

## 5.4. Pull-out test results [7, 8]

Fig. 15 shows the decohesion stress plotted versus time of treatment. Two types of curve can be seen, the first shows a monotonic increase, whereas the second curve exhibits a maximum.

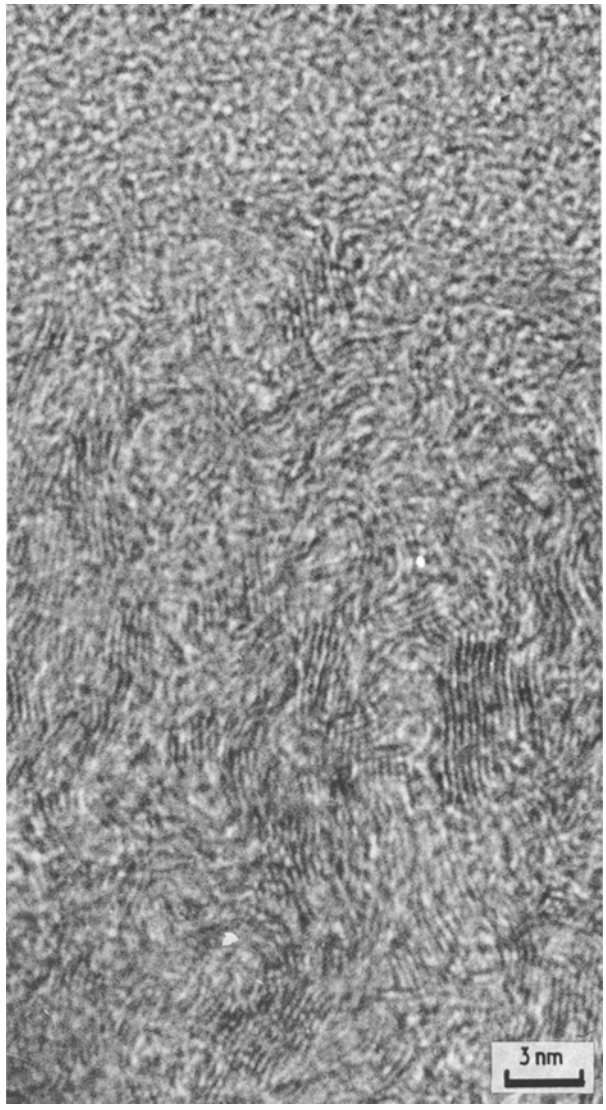


*Figure 11* High-strength carbon fibre: urea treatment.

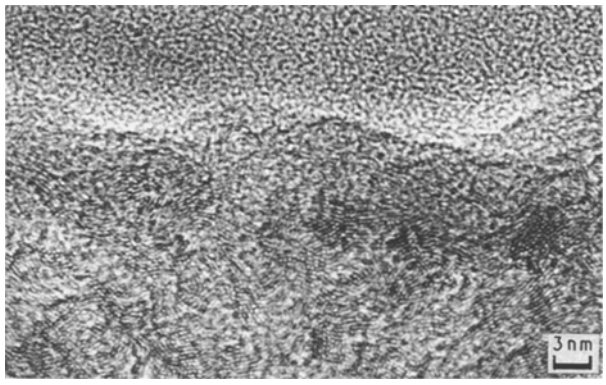


*Figure 12* High-strength carbon fibre: urea treatment.

## 6. Conclusions

1. For commercial fibres, we observed identical interphase regions.

2. The fibre–matrix adhesion was enhanced by the presence of edges of the carbon layers.

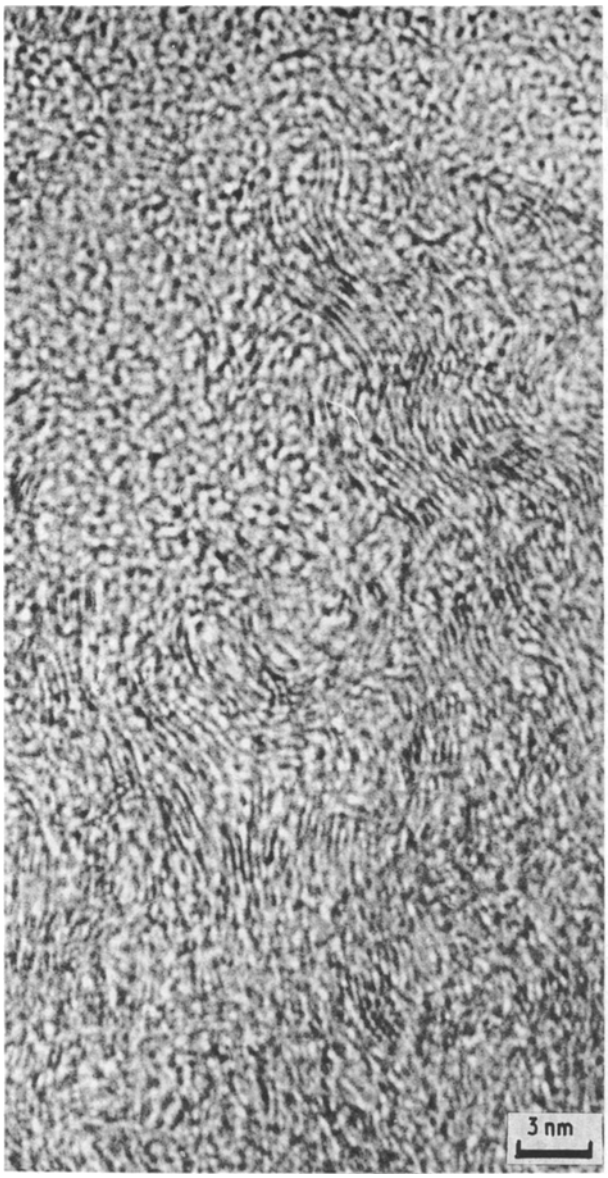


*Figure 13* High-strength carbon fibre: nitrogen plasma treatment.

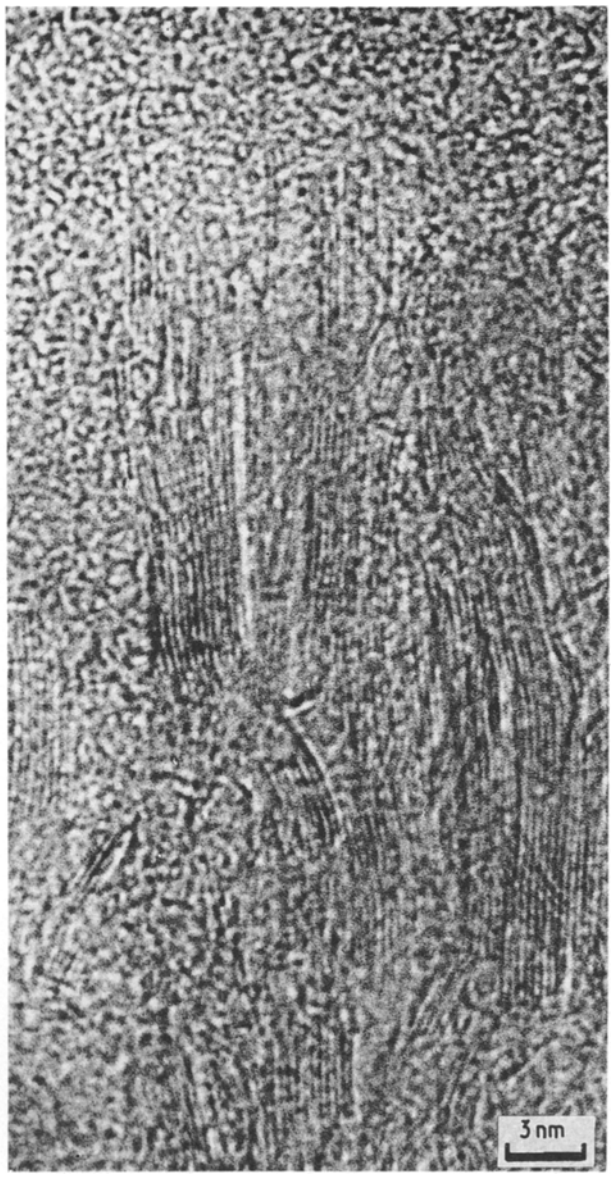


*Figure 14* High-modulus carbon fibre: nitrogen plasma treatment.

3. Long tetramine hexamethylene treatments are detrimental in obtaining a high contact ratio, but lead to a better decohesion stress.

4. We were unable to find any difference between the two treatments with urea, but the decohesion stress was higher for the longer treatment.

5. No difference was found between the contact ratio in the case of nitrogen plasma treatments. However, a long treatment gave a high decohesion stress.

These observations led us to the following conclusions.

1. In terms of large defects, mechanical hanging up does not fit in our case. However, fibre–matrix junctions are favoured by a few nanometres relief thought

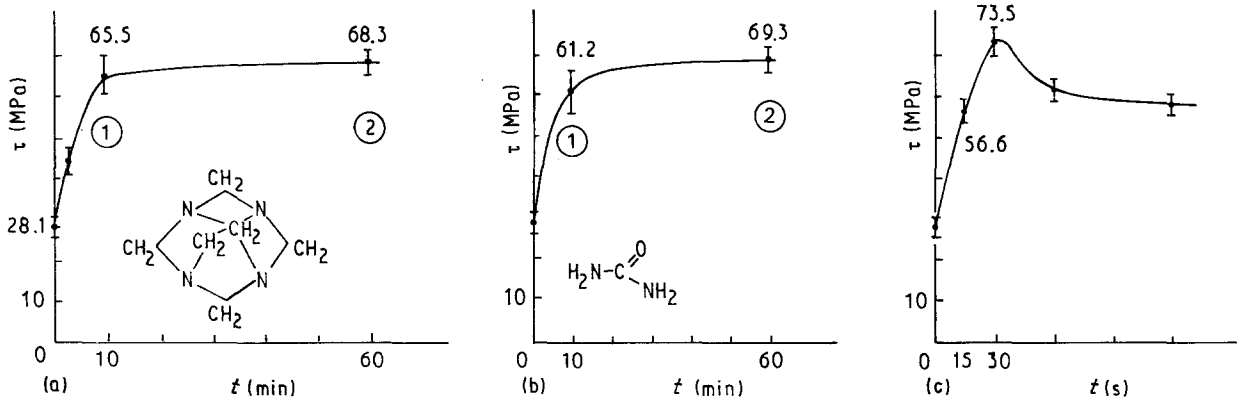


*Figure 15* Decohesion stress, $\sigma_d$, versus time of treatment, $t$, in (a) tetramine hexamethylene, (b) urea, (c) nitrogen-high strength fibre.

to be produced by treatments which attack the weakly linked carbon atoms. In fact, the convex areas of the interface are under tension and are, via their defects sensitive to all attacks. The erosion of a dome exposes many carbon layer edges which outcrop on the surface. In this process, it is likely that the indented surface is the step preceding the presence of concave and convex areas for the high-strength fibres.

2. The decohesion stress depends on the contact index which itself depends on the accessibility of the carbon layers at the interface (edge or surface). In fact, we know that the decohesion stress is $\tau_d = F/pl$ where $F$ is the decohesion force for a fibre–matrix contact surface equal to $pl$, $p$ being the fibre perimeter. We have defined $C = \Sigma a_i/p$, thus $\tau_d = f(C)$. Unfortunately, we have not obtained contact index values with a sufficient accuracy.

3. The nitrogen plasma treatment (1 min) of the high-modulus fibre leads to a decohesion stress of 66.5 MPa (15.2 MPa for the untreated fibre) corresponding to the maximal value observed for the high-strength fibre. As in all cases of poor contact in relation to a high decohesion stress, we think that only a few active sites (probably fixed on the edges of the carbon layers) are sufficient to promote a strong fibre–matrix bonding and consequently to give a high value of stress decohesion.

4. It should be noted that a good contact index is found in relation to the monotonic curves, whereas a small contact index is found in relation with the curves exhibiting a maximum. We can compare our observations with the results of the pull-out test (poor contact index–high decohesion stress) if we admit that a few strong bondings are sufficient to ensure a high decohesion stress. Strong bondings take place with the active sites fixed on the edges of carbon layers (perpendicular to the interface) scattered at the fibre surface (diffused interface). On the contrary, reliable bondings are found between the carbon layers (parallel to the interface), whose defect areas are slightly attacked (clear interface).

5. No interphase was observed for the unsized fibres. The interphase detected for the commercially sized fibres may be connected to the reaction described by Fitzer *et al.* [16].

6. The lattice fringe images are particularly well adapted for characterizing the morphology of the fibre–matrix interface in a composite material. In particular, they allow us to determine the nature (clear or diffused) of the interface related to the orientations of the carbon layers at the surface of the fibre (parallel or perpendicular).

7. The relation between the interface morphology and the decohesion stress is not well established. Certainly the fibre–matrix interpenetration is an essential condition for good adhesion. This condition leads to the establishment of a diffused interface [17] that would be controlled for a given function of a composite. In fact, it is possible that a high strength is controlled by a diffused interface, whereas a high resilience is controlled by a clear interface [18].

## Acknowledgements

The author acknowledges the support of DRET, CNRS and ONERA (M. Desarmot).

## References

1. G. D. ANDREEVSKAIA and C. V. SHIRIAJEVA *Polym. Sci. USSR* **5** (1964) 854.
2. L. J. BROUTMAN, *Polym. Engng Sci.* **6** (1966) 263.
3. L. J. BROUTMAN, "Interfaces in composites" *ASTM STP*, **452** (1969) 27.
4. J. P. FAVRE and M. C. MERIENNE, *Int. J. Adhesion Adhesives* **10** (1981) 311.
5. J. P. FAVRE and J. PERRIN, *J. Mater. Sci.* **7** (1972) 1113.
6. A. T. DI BENEDETTO and L. NICOLAIS, *Plast.* **10** (1979) 83.
7. M. SANCHEZ, Thesis, University of Paris VI (1986).
8. M. SANCHEZ, G. DESARMOT, M. C. MERIENNE and B. BARBIER, in "Proceedings of the 5th National Conference on Composites", edited by C. Bathias and D. Menkes, Pluralis, Paris (AMAC, 1986) p. 472.
9. M. R. PIGGOTT, *Compt. Sci. Tech.* **30** (1987) 295.
10. A. LANNES and J. Ph. PEREZ, "Optique de Fourier en microscopie électronique" (Masson, Paris, 1983).
11. M. GUIGON, Thèse d'Etat, Université de Technologie de Compiègne (1985).
12. W. WALTERSSON, *Compt. Sci. Tech.* **23** (1985) 303.
13. M. GUIGON, A. OBERLIN and G. DESARMOT, *Fibre Sci. Technol.* **20** (1984) 55.
14. *Idem., ibid.* **20** (1984) 177.
15. L. T. DRZAL, *SAMPE J.* **7** (September/October) (1983) 7.
16. E. FITZER, K. M. GEIGL, W. HUTTNER and R. WEISS, *Carbon* **18** (1980) 389.
17. P. G. DE GENNES, *C.R. Acad. Sci. Paris Série II* **308** (1989) 13.
18. M. GUIGON, *Microsc. Microanal. Microstruct.* **2** (1991) 15.

*Received 4 June 1990*
*and accepted 31 January 1991*